

# Symmetry, Multistability, and Long-Range Interactions in Brain Development

Fred Wolf

*MPI for Dynamics and Self-Organization, D-37073 Göttingen, Germany*  
*Bernstein Center for Computational Neuroscience, University of Göttingen, Göttingen, Germany*  
*Kavli Institut for Theoretical Physics, UCSB, Santa Barbara, California, USA*  
 (Received 23 August 2004; published 7 November 2005)

An analytically tractable class of dynamical models for the pattern of contour detecting neurons in the visual cortex is introduced. A permutation symmetry of the model equations guarantees the emergence of contour detectors for all stimulus orientations. By this symmetry a large number of dynamically degenerate solutions exist that quantitatively reproduce the experimentally observed patterns. Long-range interactions are essential for the stability of these realistic solutions.

DOI: 10.1103/PhysRevLett.95.208701

PACS numbers: 87.19.La, 05.65.+b, 42.66.Si, 47.54.+r

It is a long-standing hypothesis that the architecture of the brain's visual cortex, which underlies our ability to see, emerges through a dynamical, learning driven process [1]. In the young brain, neural activity and visual experience guide a continuous refinement of neuronal circuits by synaptic plasticity, the basic neuronal learning mechanism [2]. It has been proposed to model the resulting progressive refinement of the visual cortical architecture by a dynamics of visual cortical selectivity patterns [3–7]. Within this framework, spontaneous symmetry breaking explains how cortical neurons initially exhibiting relatively unselective responses become selective for specific features of visual stimuli [3]. After symmetry breaking, ongoing improvement may result in the convergence of the cortical architecture to a stable stationary state [4], constituting an attractor of the visual system's learning dynamics. Because the development of the visual cortical architecture is in many respects reminiscent of dynamical pattern formation in physical systems far from equilibrium [8], it is natural to ask whether this process might be modeled by dynamical equations for macroscopic order parameters, as often proved successful and instructive in simpler pattern formation problems.

In this Letter, I introduce an analytically tractable class of model equations for the formation of the spatial pattern of contour detecting neurons in the visual cortex, called the orientation preference map (OPM). Functional brain imaging has revealed that the spatial structure of OPMs is aperiodic but roughly repetitive with a characteristic wavelength in the millimeter range (see, e.g., Ref. [9]) and that OPMs contain numerous singular points, called pinwheel centers [10] [Fig. 1(b)]. The class of model equations introduced in the following has solutions that qualitatively and quantitatively resemble the experimentally observed patterns. Its construction is based on the requirement that the visual cortex must develop detectors for contours of all orientations. Assuming a supercritical bifurcation, this is guaranteed near criticality by a permutation symmetry of the model equations. This symmetry implies the existence of a large number of dynamically degenerate solutions that are qualitatively very similar to OPMs in the visual cortex.

Further analysis reveals that, judged by their pinwheel densities, these patterns even quantitatively resemble experimentally observed OPMs. The stability boundaries of various solutions are calculated in a simple model equation incorporating long-range interactions, a key feature of visual cortical processing. Long-range interactions are found to be essential for the stability of realistic solutions.

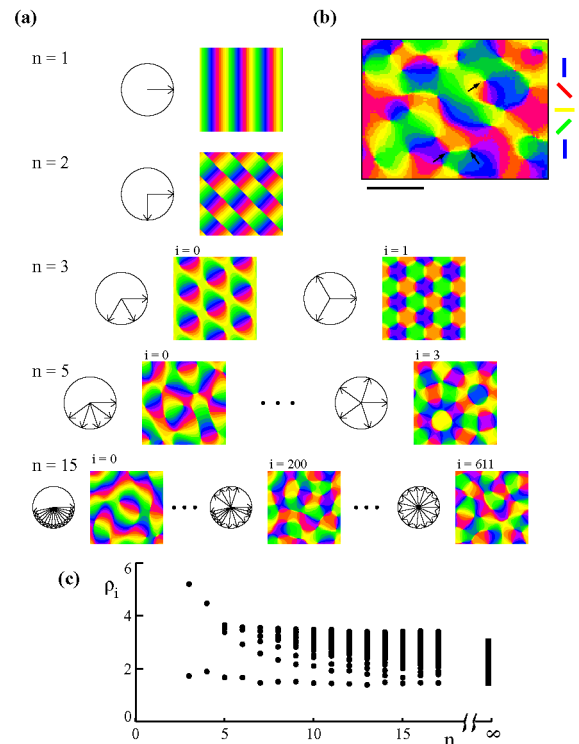


FIG. 1 (color online). (a) ECPs. Preferred stimulus orientations are color coded [see bars in (b)]. Diagrams show positions of active mode wave vectors. For  $n = 3, 5$ , and  $15$ , there are 2, 4, and 612 different ECPs, respectively. (b) Orientation preference map in cat area 17 (data: S. Löwel, IfN Magdeburg, Germany). Arrows pinwheel centers. Scale bar 1 mm. (c) Pinwheel densities (dots) of ECPs for  $n = 3-17$  ( $\Lambda = 1$ ). Bar: band of pinwheel densities for  $n \rightarrow \infty$ .

The spatial structure of an OPM can be completely characterized by a complex valued field  $z(\mathbf{x})$  where  $\mathbf{x}$  denotes the 2D position of neurons in the visual cortex,  $\vartheta(\mathbf{x}) = \arg(z(\mathbf{x}))/2$  their preferred stimulus orientation, and the modulus  $|z(\mathbf{x})|$  is a measure of their selectivity [3]. In this representation, pinwheel centers are zeros of the field  $z(\mathbf{x})$ . The simplest models for the formation of OPMs are defined by a dynamics of the field  $z(\mathbf{x}, t)$

$$\partial_t z(\mathbf{x}, t) = F[z(\cdot, t)], \quad (1)$$

where  $t$  denotes time and  $F[z(\cdot, t)]$  is a nonlinear operator. This operator represents the average change of the OPM induced by an ensemble of activity patterns [4]. It is hypothesized that the refinement of the visual cortical architecture represents an optimization process. To incorporate this hypothesis, only variational dynamics are considered in the following. Boundary effects are neglected by considering a cortical area of infinite size.

The dynamics Eq. (1) can be characterized by symmetry assumptions and the phenomenology of cortical development. Within the cortical layers there are no special locations or directions [11]. The operator  $F[z(\cdot, t)]$  should thus be equivariant under translations  $\hat{T}_y z(\mathbf{x}) = z(\mathbf{x} + y)$  and rotations  $\hat{R}_\beta z(\mathbf{x}) = e^{2i\beta} z(\Omega_\beta \mathbf{x})$  with rotation matrix  $\Omega_\beta$  [7]. For simplicity, symmetry under global shifts of preferred orientation  $F[e^{i\phi} z] = e^{i\phi} F[z]$  is also assumed. These assumptions imply that the homogeneous unselective state  $z(\mathbf{x}) = 0$  is a fixed point and that a power series representation of  $F[z]$  contains odd terms only:

$$F[z] = \hat{L}z + N_3(z, z, \bar{z}) + N_5(z, z, \dots) + \dots \quad (2)$$

In Eq. (2) these are written using  $(2i + 1)$ -argument operators  $N_{2i+1}(v_1, v_2, \dots, v_{2i+1})$  linear in each argument. The orientation shift symmetry implies that  $(i + 1)$  of these arguments are  $z$ , whereas the remaining  $i$  are its conjugate,  $\bar{z}$ . Experimentally, it is observed that OPMs emerge from an initial state of relatively low selectivity  $z_{\text{init}}(\mathbf{x}) \approx 0$  and early on exhibit wavelengths similar to that of the final state [12]. This behavior is reproduced if Eq. (1) exhibits a finite wavelength instability, i.e., if the spectrum of eigenvalue  $\lambda(k)$  of the linear operator  $\hat{L}$  exhibits a single positive maximum  $r = \lambda(k_c) > 0$  at nonzero critical wave number  $k_c$ . Simple model equations fulfilling this requirement are thus of the Swift-Hohenberg (SH)-type with  $\hat{L}_{\text{SH}} = [r - (k_c^2 + \nabla^2)^2]$ .

The dynamics Eq. (1) describes the formation of a map that contains all orientations. It is, however, easy to see that this equation always has stationary solutions that are real valued or—more generally—contain only two orientations. If such solutions were stable, the developmental dynamics might then lead to the formation of a system blind to most stimulus orientations. Because it is a fundamental requirement that the visual cortex must develop detectors for all orientations, these solutions ought to be unstable in every plausible candidate model.

Interestingly, if the bifurcation is supercritical, this fundamental requirement can be satisfied near criticality ( $r \ll 1$ ) by the permutation symmetry

$$N_3(u, v, w) = N_3(w, u, v). \quad (3)$$

This is found by considering the stability of planforms  $z(\mathbf{x}) = \sum_{j=1}^n A_j e^{i\mathbf{k}_j \mathbf{x}}$  with an even number  $n$  of active modes with amplitudes  $A_j$  and  $\mathbf{k}_j = k_c(\cos(2\pi j/n), \sin(2\pi j/n))$ . By symmetry, the dynamics of the amplitudes  $A_j$  at threshold has the form

$$\dot{A}_i = A_i - \sum_{j=1}^n g_{ij} |A_j|^2 A_i - \sum_{j=1}^n f_{ij} A_j A_{j^-} \bar{A}_{i^-}, \quad (4)$$

where  $j^-$  denotes the index of the mode antiparallel to mode  $j$ ,  $\mathbf{k}_{j^-} = -\mathbf{k}_j$ , and the coefficients  $g_{ij} = (1 - \frac{1}{2}\delta_{ij}) \times g(|\alpha_i - \alpha_j|)$  and  $f_{ij} = (1 - \delta_{ij} - \delta_{i^-j}) f(|\alpha_i - \alpha_j|)$  depend only on the angles  $|\alpha_i - \alpha_j|$  between modes  $i$  and  $j$ . Equation (4) have solutions representing only two contour orientations. For instance, there are real valued solutions  $A_j = a_0 e^{i\phi_j}$  with  $\phi_j = -\phi_{j^-}$  and  $a_0^{-2} = \sum_j (g_{ij} + f_{ij})$  containing only two orientations, horizontal and vertical. The angle-dependent interaction functions  $g(\alpha)$  and  $f(\alpha)$  are obtained from  $F[z]$  by a multiscale expansion [8] as

$$g(\alpha) = -e^{-i\mathbf{k}_0 \mathbf{x}} [N_3(e^{i\mathbf{k}_0 \mathbf{x}}, e^{i\mathbf{h}(\alpha) \mathbf{x}}, e^{-i\mathbf{h}(\alpha) \mathbf{x}}) + N_3(e^{i\mathbf{h}(\alpha) \mathbf{x}}, e^{i\mathbf{k}_0 \mathbf{x}}, e^{-i\mathbf{h}(\alpha) \mathbf{x}})], \quad (5)$$

$$f(\alpha) = -\frac{1}{2} e^{-i\mathbf{k}_0 \mathbf{x}} [N_3(e^{i\mathbf{h}(\alpha) \mathbf{x}}, e^{-i\mathbf{h}(\alpha) \mathbf{x}}, e^{i\mathbf{k}_0 \mathbf{x}}) + N_3(e^{-i\mathbf{h}(\alpha) \mathbf{x}}, e^{i\mathbf{h}(\alpha) \mathbf{x}}, e^{i\mathbf{k}_0 \mathbf{x}})], \quad (6)$$

where  $\mathbf{k}_0 = k_c(1, 0)$  and  $\mathbf{h}(\alpha) = k_c(\cos(\alpha), \sin(\alpha))$ . Both functions are assumed to be positive. Whereas  $f(\alpha)$  is  $\pi$  periodic,  $g(\alpha)$  is  $2\pi$  periodic in general. The permutation symmetry Eq. (3), however, implies  $g(\alpha) = g(\alpha + \pi)$ .

The instability of two orientation solutions in permutation symmetric models follows from the fact that with permutation symmetry the interaction function  $g(\alpha)$  is  $\pi$  periodic. Writing the moduli of the amplitudes  $|A_j| = a_0 + \delta a_j$ , the linearized dynamics of the deviations  $\delta a_j$  is  $\delta \dot{a}_i = -a_0^2 \sum_j \hat{g}_{ij} \delta a_j$  with  $\hat{g}_{ij} = 2g_{ij} + f_{ij} + f_{i^-j^-} + \delta_{i^-j^-} \sum_k f_{ik}$ . If a pair of modes  $(i, j)$  satisfies  $\hat{g}_{ij} > \hat{g}_{ii}$ , then the matrix  $\hat{g}_{ij}$  has a negative eigenvalue implying that the two orientation solution is unstable. To demonstrate the instability of two orientation solutions, consider a pair of antiparallel modes  $j = i^-$ . For such a pair, the instability condition is fulfilled if  $g_{i^-i^-} = g(\pi) > g_{ii} = g(0)/2$ . With  $g(\pi) = g(0)$  this holds in general, and the pathological two orientation solutions are unstable. As shown in the following, all orientations are contained in stable solutions of permutation symmetric models.

What are potential attractors of a permutation symmetric dynamics? At criticality, a large set of candidate solutions is given by the planforms  $z(\mathbf{x}) = \sum_j A_j e^{i\mathbf{k}_j \mathbf{x}}$  with  $n$  wave vectors  $\mathbf{k}_j = k_c(\cos(j\pi/n), \sin(j\pi/n))$  ( $j = 1, \dots, n$ ) distributed equidistantly on the upper half of the critical circle

and binary variables  $l_j = \pm 1$  determining whether the mode with wave vector  $\mathbf{k}_j$  or with wave vector  $-\mathbf{k}_j$  is active. These planforms cannot realize a real valued function and are called essentially complex planforms (ECPs) in the following. Representative examples of uniform ECPs ( $|A_j| = a_0$ ) are displayed in Fig. 1(a). For  $n \geq 3$  there are multiple planforms for fixed  $n$  that are not related by symmetry operations and each planform exhibits a large number of pinwheels with pinwheel densities differing among planforms. For  $n \geq 4$  the patterns are spatially quasiperiodic resembling experimentally observed OPMs [Fig. 1(b)] for  $n \geq 10$ .

Permutation symmetric models exhibit a potentially exceedingly high number of multistable solutions. This is revealed by examining the stability of ECPs to uniform perturbations. For an ECP, the third term of the general amplitude equations Eq. (4) vanishes and the effective amplitude equations for the active modes reduce to a system of Landau equations  $\dot{A}_i = A_i - \sum_j g_{ij} |A_j|^2 A_i$ . By Eq. (3), its coefficients  $g_{ij} \propto g[(i-j)\pi/n + (l_j - l_i)\pi/2] = g[(i-j)\pi/n]$  are independent of the variables  $l_j$  that identify a particular ECP. Consequently, the stationary amplitudes  $|A_j| = a_0 = (\sum_j g_{ij})^{-1/2}$  of all ECPs with  $n$  active modes ( $n$ -ECPs) and their internal stability properties are identical at criticality. This is found also for their energies  $U_n = -\frac{n}{4} / \sum_j g_{ij}$ , which depend only on the coefficients  $g_{ij}$ , and for their external stability [13]. Thus, although different  $n$ -ECPs can differ substantially in spatial layout including the density of pinwheel defects, the permutation symmetry Eq. (3) implies that they have degenerate energies and stability properties. As a consequence, if one  $n$ -ECP is stable, all others are stable as well.

Intuitively, ECPs with a relatively large number of active modes mimic OPMs in the visual cortex even quantitatively. Pinwheel densities  $\rho$  of visual cortical OPMs range mostly between 2–3.5 in units  $\Lambda^{-2}$  and exhibit a considerable degree of interindividual variability [14].

The pinwheel densities  $\rho_i$  of various ECPs are shown in Fig. 1(c). The pinwheel densities of ECPs can be exactly evaluated in the large  $n$  limit, because for  $n \rightarrow \infty$  local, linear functionals of  $z(\mathbf{x})$  have Gaussian statistics. The pinwheel density of an  $n$ -ECP then is  $\rho(\zeta) = \sqrt{\pi^2 - 8\zeta^2}$  and depends through  $\zeta = \frac{1}{4n} |\sum_j l_j \mathbf{k}_j| \leq 1$  on the configuration  $l_j$  of the active modes, which highlights strong variability among different  $n$ -ECPs. Figure 1(c) shows that for  $n \approx 15$  pinwheel densities fill a band of values between 1.5 and 3.5 with the majority of values between 2 and 3.5. Thus, quantitatively, pinwheel densities of ECPs with an intermediate to large number of active modes agree very well with the experimentally observed range. Because by permutation symmetry no  $n$ -ECP is energetically favored, permutation symmetric models offer a natural explanation for the experimentally observed substantial variability of pinwheel densities.

To reveal in which kind of model large  $n$ -ECPs are dynamically selected, it is instructive to consider a simple

model equation. To select a biologically plausible form of the nonlinearity, assume that  $N_3[z(\mathbf{x})]$  can be decomposed into a local component  $N_3^{\text{loc}} \propto |z(\mathbf{x})|^2 z(\mathbf{x})$  and a nonlocal component  $N_3^{\text{nl}}[z(\mathbf{x})] \propto \int d^2y [z(\mathbf{y}) - z(\mathbf{x})] W(\mathbf{x}, \mathbf{y}|z)$  with a positive definite connectivity function  $W(\mathbf{x}, \mathbf{y}|z)$  measuring the coupling strength of neurons at locations  $\mathbf{y}$  and  $\mathbf{x}$  given the OPM,  $z$ . Choosing  $W \propto \exp(-\frac{|\mathbf{y}-\mathbf{x}|^2}{2\sigma^2} - \frac{|z(\mathbf{y})-z(\mathbf{x})|^2}{\sigma_z^2})$  mimics the patchy orientation-selective long-range connectivity of visual cortical neurons while neglecting the effects of axial selectivity [15]. The relevant third order terms can then be cast in the form

$$N_3[z(\mathbf{x})] = (1-g)|z(\mathbf{x})|^2 z(\mathbf{x}) - \frac{2-g}{2\pi\sigma^2} \times \int d^2y \left( |z(\mathbf{y})|^2 z(\mathbf{x}) + \frac{1}{2} z(\mathbf{y})^2 \bar{z}(\mathbf{x}) \right) e^{-|\mathbf{y}-\mathbf{x}|^2/2\sigma^2} \quad (7)$$

where the nonlocal term is a cubic two point operator that satisfies all four symmetries and has the energy functional  $\int d^2x d^2y [ |z(\mathbf{x})z(\mathbf{y})|^2 + \frac{1}{2} z(\mathbf{x})^2 \bar{z}(\mathbf{y})^2 ] e^{-|\mathbf{y}-\mathbf{x}|^2/2\sigma^2}$ . In Eq. (7) the parameter  $\sigma$  is the range of nonlocal interactions and the coupling parameter  $g$  determines whether the local ( $g > 1$ ) or the nonlocal term ( $g < 1$ ) stabilizes the dynamics. The resulting angle-dependent interaction functions are  $g(\alpha) = g + (2-g)e(\alpha)$  and  $f(\alpha) = \frac{1}{2}g(\alpha)$  with  $e(\alpha) = 2 \exp(-\sigma^2 k_c^2) \cosh(\sigma^2 k_c^2 \cos(\alpha))$ .

Large  $n$ -ECPs are selected if the dynamics is stabilized by long-range nonlocal interactions ( $g < 1$ ,  $\sigma > \Lambda$ ). This is illustrated in Fig. 2 by numerical simulations of the Swift-Hohenberg model  $\partial_t z = \hat{L}_{\text{SH}} z + N_3[z]$  defined by Eq. (7). In Fig. 3 the regions of parameter space in which  $n$ -ECPs exhibit minimum energy are displayed. Whereas for  $g > 1$  and for short-ranged interactions pinwheel-free stripe patterns exhibit minimal energy, they lose stability at a critical line  $g_1^*(\sigma)$ . Below this critical line,  $n$ -ECPs with several active modes are stable and exhibit minimal energy.

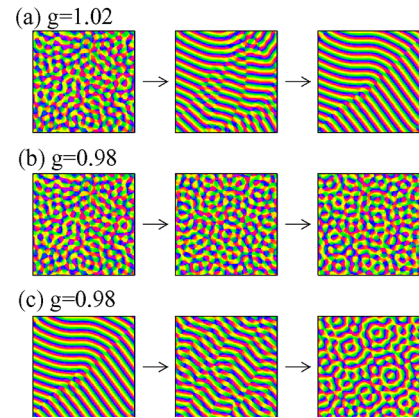


FIG. 2 (color online). Transition to pinwheel-rich ECP attractors at  $g = 1$  in the long-range regime ( $\sigma = 3\Lambda$ ). (a)–(c) Numerically obtained solutions of the SH model Eq. (7). Initial conditions identical in (a) and (b); (c) starts from the final state of (a).

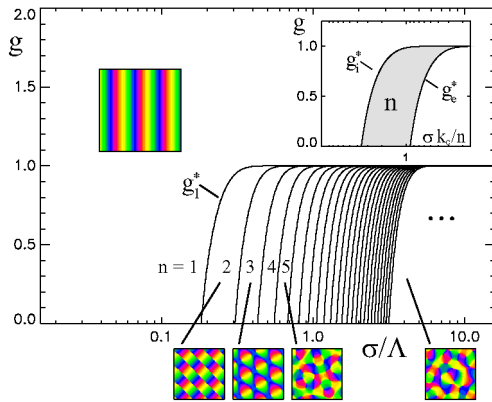


FIG. 3 (color online). Phase diagram of the SH model Eq. (7) near criticality. The graph shows the regions of the  $g$ - $\sigma/\Lambda$  plane in which  $n$ -ECPs have minimal energy ( $n = 1-25$ ,  $n > 25$  dots). Inset: stability region of  $n$ -ECPs for  $n \gg 1$ .

In the long-range regime, the number of active modes of stable  $n$ -ECPs grows linearly with the interaction range  $n_{\text{stab}} \approx 2\pi\sigma/\Lambda$ . This is found by considering the stability domains of  $n$ -ECPs in the large  $n$  limit. The domains of stability of  $n$ -ECPs are bounded by two instabilities. First,  $n$ -ECPs can become internally unstable with respect to amplitude perturbations of the active modes. Second,  $n$ -ECPs can become externally unstable with respect to the growth of additional modes on the critical circle. The corresponding stability borders  $g_i^*$  and  $g_e^*$  bound the stability region towards low values and high values of the interaction range  $\sigma$ , respectively. For  $n \gg 1$ , these stability borders are given by  $g_e^*(\sigma k_c/n) = 1 - (e^{(\pi^2/8)(\sigma k_c/n)^2}/2 - 1)^{-1}$  and  $[2 - g_i^*(\sigma k_c/n)]^{-1} = \sqrt{\frac{2}{\pi}} \frac{n}{\sigma k_c} \times \sum_{j=-\infty}^{\infty} e^{-2(j-1/2)^2(n/\sigma k_c)^2}$  with  $n$ -ECPs stable for  $g_i^*(\sigma k_c/n) > g > g_e^*(\sigma k_c/n)$  (inset of Fig. 3) [13]. Because of the dynamical degeneracy of different  $n$ -ECPs, this also implies that for  $g < 1$  the number of attractors grows combinatorially with increasing interaction range.

What does the theory presented above teach us about visual cortical development? First, it demonstrates that the formation of spatially irregular OPMs can be successfully modeled as a dynamical optimization process. In homogeneous, spatially extended systems, relaxation towards the minima of an energy functional often implies the emergence of regular states exhibiting long-range order [8]. The seemingly disordered structure of OPMs might thus be taken to indicate that frozen randomness rather than a functional optimization principle governs the layout of the maps. In fact, in many optimization models considered in the past irregular states only occur transiently and with progressive relaxation decay either to pinwheel-sparse states [4] or to crystalline arrangements of stable pinwheels [5]. The model class introduced above intrinsically possesses a multitude of spatially aperiodic solutions of realistic defect densities demonstrating that such states can be produced and sustained by optimization. Second, the

theory predicts that long-range intracortical interactions shape the spatial layout of OPMs. The example analyzed highlights the fact that in this model class realistic solutions are selected near criticality only if long-range effective interactions are present in the dynamics. Finally, the theory predicts a novel discrete multistability of visual cortical pattern formation. It is intimately linked to the functional requirement of representing *all* stimulus orientations. This kind of multistability might have profound implications for visual development and plasticity. If it is exhibited by visual cortical circuits, biological factors influencing cortical development such as genetic information, spontaneous activity patterns, and visual experience cannot *write* arbitrarily structured orientation representations but have to *choose* from a discrete repertoire of stable patterns that is an emergent collective property of the cortical learning dynamics.

I thank M. Kardar, S. Löwel, M. Kaschube, M. Schnabel, and H. Dinse for discussions. This research was supported by HFSP, VolkswagenStiftung, and MPG.

- [1] M. C. Crair, *Curr. Opin. Neurobiol.* **9**, 88 (1999); L. C. Katz and J. C. Crowley, *Nat. Rev. Neurosci.* **3**, 34 (2002).
- [2] W. Singer, *Science* **270**, 758 (1995); L. C. Katz and J. C. Shatz, *Science* **274**, 1133 (1996); F. Sengpiel and P. C. Kind, *Curr. Biol.* **12**, R818 (2002).
- [3] K. D. Miller, in *Handbook of Brain Theory and Neural Networks*, edited by M. A. Arbib (MIT Press, Cambridge, MA, 1996); N. V. Swindale, *Network* **7**, 161 (1996).
- [4] F. Wolf and T. Geisel, *Nature (London)* **395**, 73 (1998); *Lect. Notes Phys.* **527**, 174 (1999).
- [5] A. A. Koulakov and D. B. Chklovskii, *Neuron* **29**, 519 (2001).
- [6] H. Y. Lee *et al.*, *Proc. Natl. Acad. Sci. U.S.A.* **100**, 16036 (2003); M. W. Cho and S. Kim, *Phys. Rev. Lett.* **92**, 018101 (2004).
- [7] P. J. Thomas and J. D. Cowan, *Phys. Rev. Lett.* **92**, 188101 (2004).
- [8] M. C. Cross and P. C. Hohenberg, *Rev. Mod. Phys.* **65**, 851 (1993); P. Manneville, *Dissipative Structures and Weak Turbulence* (Academic Press, San Diego, CA, 1990).
- [9] S. Löwel *et al.*, *J. Comp. Neurol.* **255**, 401 (1987).
- [10] T. Bonhoeffer and A. Grinvald, *Nature (London)* **353**, 429 (1991).
- [11] V. Braitenberg and A. Schüz, *Cortex: Statistics and Geometry of Neuronal Connectivity* (Springer, Berlin, 1998).
- [12] B. Chapman *et al.*, *J. Neurosci.* **16**, 6443 (1996); M. C. Crair *et al.*, *Science* **279**, 566 (1998).
- [13] F. Wolf, Ph.D. thesis, Goethe University, Frankfurt, Germany, 1999; F. Wolf, in *Methods and Models in Neurophysics*, Proceedings of the Les Houches Summer School, Session LXXX, edited by C. C. Chow *et al.* (Elsevier, Amsterdam, 2005).
- [14] A. Shmuel and A. Grinvald, *Proc. Natl. Acad. Sci. U.S.A.* **97**, 5568 (2000); T. Müller *et al.*, *Neural Comput.* **12**, 2573 (2000);
- [15] C. D. Gilbert and T. N. Wiesel, *J. Neurosci.* **9**, 2432 (1989); W. H. Bosking *et al.*, *J. Neurosci.* **17**, 2112 (1997).